

Metformin alters the gut microbiome of individuals with treatment-naive type 2 diabetes, contributing to the therapeutic effects of the drug

Hao Wu^{1,12}, Eduardo Esteve^{2-4,12}, Valentina Tremaroli¹, Muhammad Tanweer Khan¹, Robert Caesar¹, Louise Mannerås-Holm¹, Marcus Ståhlman¹, Lisa M Olsson¹, Matteo Serino⁵, Mercè Planas-Fèlix⁶, Gemma Xifra²⁻⁴, Josep M Mercader⁶, David Torrents^{6,7}, Rémy Burcelin^{8,9}, Wifredo Ricart²⁻⁴, Rosie Perkins¹, José Manuel Fernández-Real²⁻⁴ & Fredrik Bäckhed^{1,10,11}

Metformin is widely used in the treatment of type 2 diabetes (T2D), but its mechanism of action is poorly defined. Recent evidence implicates the gut microbiota as a site of metformin action. In a double-blind study, we randomized individuals with treatment-naive T2D to placebo or metformin for 4 months and showed that metformin had strong effects on the gut microbiome. These results were verified in a subset of the placebo group that switched to metformin 6 months after the start of the trial. Transfer of fecal samples (obtained before and 4 months after treatment) from metformin-treated donors to germ-free mice showed that glucose tolerance was improved in mice that received metformin-altered microbiota. By directly investigating metformin–microbiota interactions in a gut simulator, we showed that metformin affected pathways with common biological functions in species from two different phyla, and many of the metformin-regulated genes in these species encoded metalloproteins or metal transporters. Our findings provide support for the notion that altered gut microbiota mediates some of metformin's antidiabetic effects.

Metformin is the most prescribed pharmacotherapy for the treatment of individuals with type 2 diabetes (T2D) because of its relative safety, low cost, and beneficial effects on blood glucose and cardiovascular mortality^{1,2}. However, its mechanism of action remains unclear. Although metformin is generally considered to mediate its antihyperglycemic effects by suppressing hepatic glucose output through the activation of AMP-activated protein kinase (AMPK)-dependent³⁻⁵ and AMPK-independent pathways⁶⁻⁸ in the liver, accumulating evidence indicates that it might also act through pathways in the gut^{9,10}. For example, its glucose-lowering effect is more pronounced when given orally than when administered intravenously¹¹. In addition, a study comparing metformin formulations with reduced and normal plasma exposure provided evidence to indicate that the lower bowel is a major site of action for metformin¹². Furthermore, recent studies in both rodents¹³⁻¹⁵ and humans¹⁶⁻¹⁸ suggest that gut microbial changes might contribute to the antidiabetic effect of metformin. So far, however, it is not known how metformin affects the gut microbiota of individuals with treatment-naive T2D, nor how metformin interacts with gut bacteria.

Here we performed a randomized, placebo-controlled, double-blind study in individuals with newly diagnosed T2D on a calorie-restricted diet, and we combined metagenomics and targeted metabolomics to investigate the effect of metformin on the composition and function of the gut microbiota. We also transferred human fecal samples to germ-free mice to study the effects of metformin-altered microbiota on host glucose metabolism, and we used an *in vitro* gut simulator to investigate metformin–microbiota interactions directly.

RESULTS

Metformin alters the gut microbiota composition

To investigate how metformin affects the composition of the gut microbiota, we randomized treatment-naive individuals with recently diagnosed T2D to receive either placebo ($n = 18$) or 1,700 mg/d of metformin ($n = 22$) for 4 months in a double-blind study. Clinical characteristics of these individuals before and after treatment are presented in **Table 1**. Both groups were recommended to consume a calorie-restricted diet for the 4-month study period (**Supplementary Table 1**); calorie intake was reduced by a median of 342 kcal/d, and

¹Department of Molecular and Clinical Medicine, Wallenberg Laboratory, Institute of Medicine, University of Gothenburg, Gothenburg, Sweden. ²Department of Diabetes, Endocrinology and Nutrition, Institut d'Investigació Biomèdica de Girona, Hospital Josep Trueta, Girona, Spain. ³Departament de Medicina, Facultat de Medicina, University of Girona, Girona, Spain. ⁴Centro de Investigación Biomédica en Red de Fisiopatología de la Obesidad y Nutrición (CIBEROBN), Instituto de Salud Carlos III, Madrid, Spain. ⁵IRSD, Université de Toulouse, INSERM, INRA, ENVT, UPS, Toulouse, France. ⁶Barcelona Supercomputing Center (BSC), Joint BSC–CRG–IRB Research Program in Computational Biology, Barcelona, Spain. ⁷Institut Catalana de Recerca i Estudis Avançats (ICREA), Barcelona, Spain. ⁸Institut National de la Santé et de la Recherche Médicale (INSERM), Toulouse, France. ⁹Université Paul Sabatier (UPS), Unité Mixte de Recherche 1048, Institut de Maladies Métaboliques et Cardiovasculaires, Toulouse, France. ¹⁰Sahlgrenska University Hospital, Gothenburg, Sweden. ¹¹Novo Nordisk Foundation Center for Basic Metabolic Research, Section for Metabolic Receptology and Enteroendocrinology, Faculty of Health Sciences, University of Copenhagen, Copenhagen, Denmark. ¹²These authors contributed equally to this work. Correspondence should be addressed to J.M.F.-R. (jmfreal@idibgi.org) or F.B. (fredrik.backhed@wlab.gu.se).

Received 27 June 2016; accepted 19 April 2017; published online 22 May 2017; doi:10.1038/nm.4345

Table 1 Clinical characteristics for the 40 individuals with T2D enrolled in this study

	Placebo group (n = 18)			Metformin group (n = 22)		
	P0	P2	P4	M0	M2	M4
Age (years)	54.9 ± 1.9	–	–	52.6 ± 2.0	–	–
Sex (male/female)	9/9	–	–	8/14	–	–
Weight (kg)	85.4 ± 5.6	82.2 ± 5.6 ⁺	81.5 ± 5.4 [#]	96.5 ± 4.1	92.9 ± 4.0	91.4 ± 3.9
Waist circumference (cm)	106.1 ± 4.4	101.7 ± 4.3 [*]	101.9 ± 3.6	111.5 ± 2.7	108.3 ± 2.9 [*]	108.7 ± 2.9
HOMA	8.0 ± 1.5	8.9 ± 1.6	8.1 ± 1.8	8.3 ± 1.2	6.2 ± 0.9	6.0 ± 0.8 [*]
Total cholesterol (mg/dl)	205.8 ± 8.8	197.8 ± 7.7	190.7 ± 6.9 [*]	206.0 ± 7.4	196.6 ± 7.2	198.8 ± 7.5
HDL-C (mg/dl)	46.9 ± 3.4	45.0 ± 3.0	46.8 ± 3.1	48.4 ± 2.7	55.2 ± 6.1	51.1 ± 3.0 [*]
LDL-C (mg/dl)	126.8 ± 6.6	124.8 ± 5.7	118.1 ± 6.2 [*]	129.4 ± 6.4	117.4 ± 6.2 [*]	121.5 ± 6.8
Triglycerides (mg/dl)	151.9 ± 18.7	155.9 ± 15.2	129.3 ± 12.5	129.0 ± 17.8	139.6 ± 11.6	135.9 ± 12.7
ALT (U/liter)	33.2 ± 7.2	24.3 ± 2.9	22.3 ± 2.1	35.5 ± 3.5	28.0 ± 1.8 ⁺	32.8 ± 3.2
GGT (U/liter)	38.4 ± 5.4	28.2 ± 2.1 ⁺	26.3 ± 2.0 ⁺	44.0 ± 6.0	31.3 ± 3.2 ⁺	34.1 ± 3.9 [*]
CRP (mg/dl)	0.4 ± 0.1	0.6 ± 0.1	0.5 ± 0.1	0.4 ± 0.1	0.4 ± 0.1	0.4 ± 0.1
Statin treatment (n)	3	–	–	4	–	–
Antihypertensive treatment (n)	2	–	–	3	–	–

ALT, alanine transaminase; CRP, C-reactive protein; GGT, γ -glutamyl transferase; HDL-C, high-density lipoprotein cholesterol; HOMA, homeostatic model assessment; LDL-C, low-density lipoprotein cholesterol. ^{*} $P < 0.05$; ⁺ $P < 0.01$; [#] $P < 0.001$ versus P0 or M0. Wilcoxon signed-rank test; data are shown as means \pm s.e.m.

no significant differences were seen between the groups ($P = 0.90$). A subset of the placebo group switched to receive metformin (850 or 1,700 mg/d; $n = 13$) 6 months after the start of the study; to validate our findings from the randomized study, we analyzed samples from this group after a further 6 months.

As expected given the reduced calorie intake, body-mass index (BMI) decreased significantly in both the placebo and metformin groups over the initial 4-month study period (Fig. 1a). However, significant decreases in % hemoglobin A1c (HbA1c) and fasting blood glucose were observed only in the group randomized to metformin treatment (Fig. 1b,c). BMI did not decrease further in the switched subgroup after 6 months on metformin (Fig. 1a), but %HbA1c and fasting blood glucose were significantly reduced by metformin in this subgroup (Fig. 1b,c).

To characterize the effects of metformin on the gut microbiome, we performed whole-genome shotgun sequencing of 131 fecal samples. On average, we obtained 38 million paired-end reads for each sample (ranging from 15 million to 116 million; Supplementary Table 2). The taxonomy and gene profiles were estimated by mapping the high-quality reads to nonredundant genome and gene catalogs implemented in the metagenomic data-utilization and analysis (MEDUSA) pipeline¹⁹, respectively. Only one bacterial strain was altered over the 4-month study period in the placebo group (Fig. 1d), despite the reduction in BMI. By contrast, metformin treatment for 2 and 4 months resulted in significant alterations in the relative abundance of 81 and 86 bacterial strains, respectively, most of which belonged to γ -proteobacteria (for example, *Escherichia coli*) and Firmicutes (Fig. 1d and Supplementary Table 3; false-discovery rate (FDR) < 0.05). At the genera level, we observed an increase of *Escherichia* and a decrease of *Intestinibacter* in the metformin-treated group (Supplementary Table 3). Notably, the microbial changes observed after 2 and 4 months of metformin treatment in our randomized study correlated with the microbial changes observed in the switched subgroup after 6 months on metformin (Fig. 1e). We also observed a metformin-induced increase in *Bifidobacterium* in this subgroup (Supplementary Table 3).

Earlier studies have shown an association between metformin and the abundance of *Akkermansia muciniphila*^{13–15,18} and between *A. muciniphila* and improved metabolic features in mice^{13,20,21} and humans²². In a targeted analysis of our metagenome data, we showed

increased abundance of *A. muciniphila* in individuals who received metformin for 4 months (Supplementary Fig. 1). However, we did not observe any significant correlations between %HbA1c and *A. muciniphila* abundance in our cohort ($P > 0.1$; Supplementary Fig. 1).

To investigate how different gut bacteria interact with each other, we performed a coabundance network analysis. We showed that 2 months of metformin treatment promoted an increased number of positive connections among microbial genera, especially those within Proteobacteria and Firmicutes (Fig. 1f). We also identified a few interphylum connections, such as between *Shewanella* (Proteobacteria) and *Blautia* (Firmicutes), a short-chain fatty acid (SCFA)-producing genus²³.

To test the effect of metformin on microbial growth, we mapped whole-genome shotgun reads to the genomes of common strains in the human gut to determine the ratio between DNA copy number near the replication origin and DNA copy number near the terminus (termed the peak-to-trough ratio, PTR) of bacterial genomes²⁴. After correction for FDR, we found that the PTR of only one bacterial species (*Bifidobacterium adolescentis*) was significantly increased by metformin (Fig. 2a). In agreement, the PTR of *B. adolescentis* was also increased in the switched subgroup after 6 months on metformin (Fig. 2a). Furthermore, in our cohort, we observed a negative correlation between the PTR of *B. adolescentis* and %HbA1c (Spearman coefficient $\rho = -0.28$, $P < 0.01$). Consistent with this observation, *in vitro* analysis showed that metformin directly promoted the growth of *B. adolescentis* in pure cultures (Fig. 2b). We also showed that metformin directly promoted the growth of *A. muciniphila*, but not of *E. coli*, in pure cultures (Fig. 2c,d).

Metformin-altered microbiota improves glucose tolerance

To investigate whether metformin-altered microbiota could contribute to the glucose-lowering effect of metformin, we transferred fecal samples from three metformin-treated participants (before and 4 months after metformin, here termed M0 and M4 microbiota) to germ-free mice. All three of the metformin recipients responded similarly to metformin in terms of reduced %HbA1c, as compared to baseline, after 2 and 4 months on metformin. The mice were fed a high-fat diet for 1 week before and during colonization for 18 d.

We did not observe any differences in body weight, body fat, or fasting insulin between mice that received M4 and M0 microbiota (Fig. 3a,b and Supplementary Fig. 2a–c). However, we found improvements

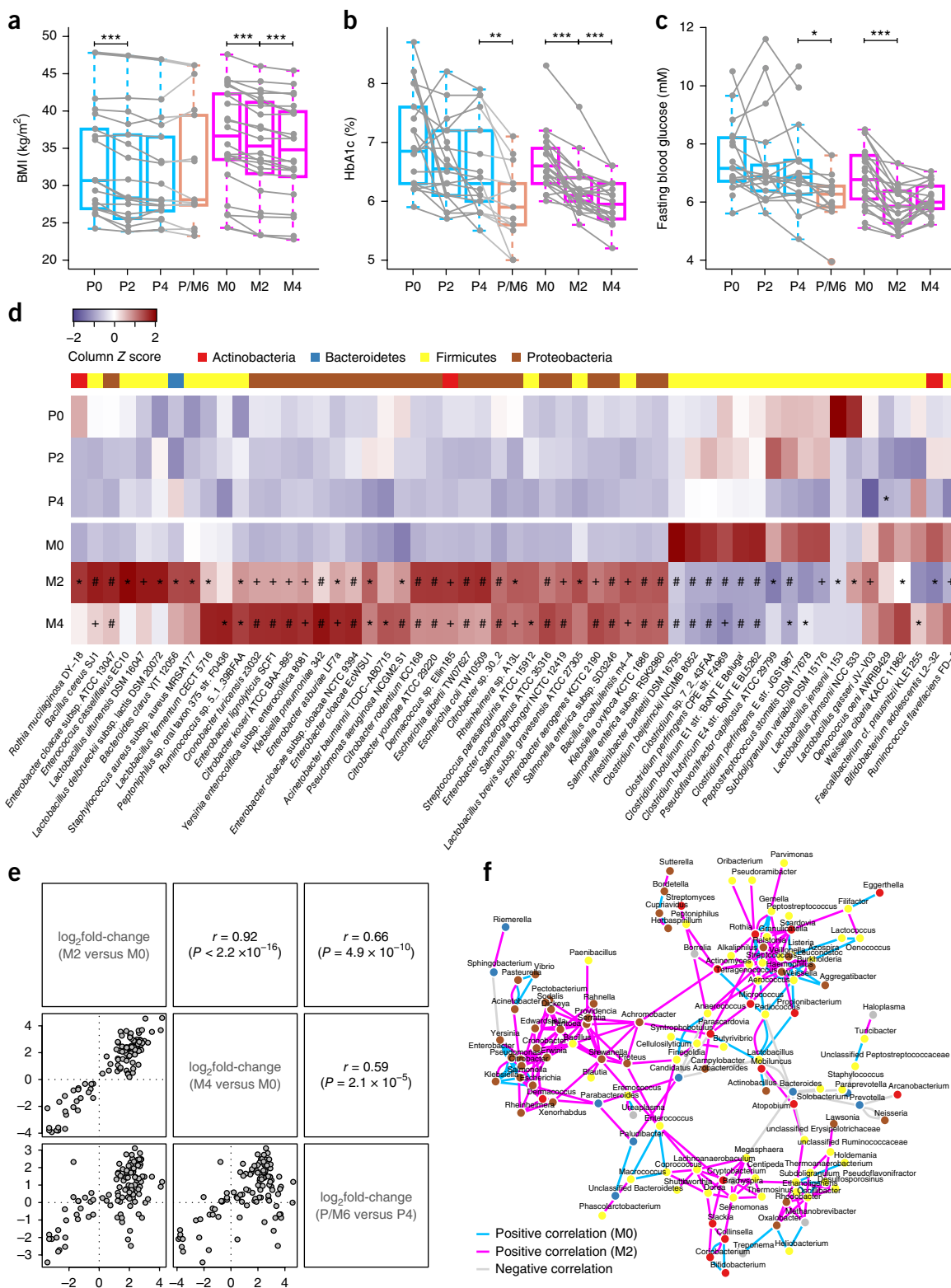


Figure 1 Metformin treatment promotes rapid changes in the composition of the gut microbiota. (**a–c**) Boxplots (with median) showing BMI, %HbA1c, and fasting blood glucose before treatment (P0 and M0) and after 2 and 4 months in individuals with T2D randomized to placebo (P2 and P4; $n = 18$) or metformin (M2 and M4; $n = 22$), and 6 months after metformin in a subgroup that switched from placebo to metformin after the randomized study period (P/M6; $n = 13$). Wilcoxon signed-rank test; * $P < 0.05$; ** $P < 0.01$; *** $P < 0.001$. (**d**) Heat map showing changes in the abundance of bacterial strains after placebo or metformin treatment (only strains with >50 reads mapped are shown). Wald test; *FDR < 0.05; +FDR < 0.01; #FDR < 0.001. (**e**) Pearson correlations between microbial changes observed at M2 as compared to M0; M4 as compared to M0; and P/M6 as compared to P4. (**f**) Genus–genus coabundance network before (M0) and after 2 months of metformin treatment (M2) in individuals with T2D. The edges indicate Spearman correlations of >0.6 or <-0.6 between genera present in at least 80% samples.

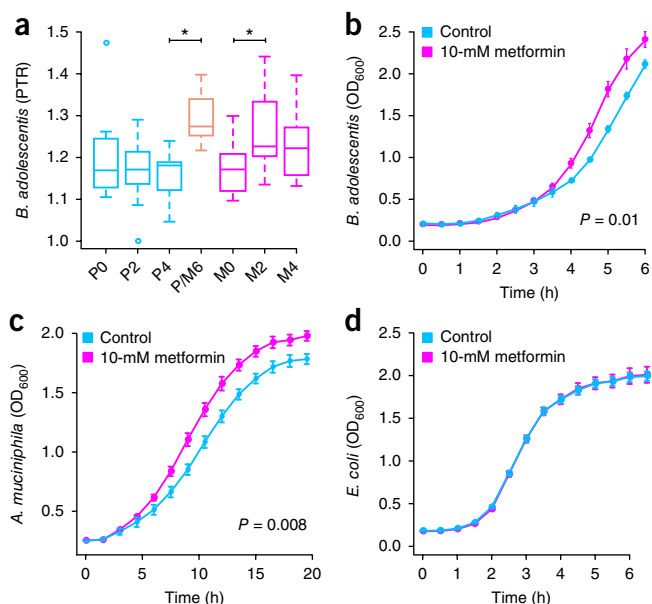


Figure 2 Metformin treatment promotes the growth of gut bacteria. (a) Boxplots (with median) showing *B. adolescentis* growth as estimated by peak-to-trough ratio (PTR) before treatment (P0 and M0) and after 2 and 4 months in individuals with T2D randomized to placebo (P2 and P4; $n = 18$) or metformin (M2 and M4; $n = 22$) and 6 months after metformin in a subgroup that switched from placebo to metformin after the randomized study period (P/M6; $n = 13$). Wilcoxon signed-rank test; *FDR < 0.05. (b–d) Growth of *B. adolescentis*, *A. muciniphila*, and *E. coli* as single cultures in the presence or absence of 10-mM metformin (with six technical replicates). P values were determined by two-way analysis of variance (ANOVA) with repeated measurements. Data are shown as means \pm s.e.m.

in glucose tolerance in mice that received M4 microbiota, as compared to those that received M0 microbiota, from two of the three donors (Supplementary Fig. 2d–f) and when combining the results from all three transfer experiments (Fig. 3c).

Metformin promotes functional shifts in the gut microbiome

To further investigate functional changes in the gut microbiome after metformin treatment, we annotated genes to Kyoto encyclopedia of genes and genomes (KEGG) orthology (KO)²⁵. Only two KOs were significantly altered over the 4-month study period in the placebo group (FDR < 0.05). By contrast, 626 and 473 KOs were increased, whereas 130 and 69 KOs were decreased after 2 and 4 months of metformin, respectively (Supplementary Fig. 3 and Supplementary Table 4; FDR < 0.05), and most of the shifts were consistent between the two sampling times (Supplementary Fig. 3). Principal coordinate analysis (PCoA) of the relative abundance of all of the significantly altered KOs revealed similar gene functions in the placebo group at all time points and the metformin group at baseline (i.e., before treatment), but we observed significant shifts after metformin treatment for 2 months and 4 months (Fig. 4a). Pathway-enrichment analysis revealed that metformin treatment was linked mainly to the enrichment of genes for bacterial environmental responses (for example, bacterial secretion system, two component system, and ATP-binding cassette (ABC) transporters), drug resistance (bacterial chemotaxis and cationic antimicrobial peptide resistance), central carbohydrate metabolism (phosphotransferase system, pyruvate, butyrate, and propionate metabolism), amino acid metabolism, and lipopolysaccharide (LPS) biosynthesis (Fig. 4b and Supplementary Table 4; FDR < 0.05).

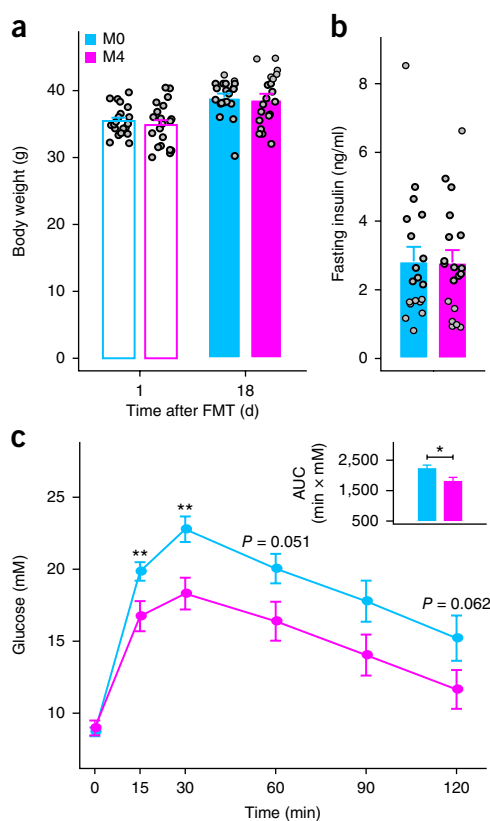


Figure 3 Metformin-altered microbiota improves glucose tolerance. (a) Body weight of mice 1 d and 18 d after colonization with fecal microbiota obtained from three individuals with T2D before (M0) and 4 months after metformin treatment (M4). (b) Fasting plasma insulin concentrations measured in the same mice used in a 18 d after colonization. (c) Plasma glucose concentrations measured in the same mice used in a during an intraperitoneal glucose-tolerance test 18 d after colonization. Data are shown as means \pm s.e.m. and are the combined results of three independent transfer experiments (shown individually in Supplementary Fig. 2). M0: $n = 20$ mice; M4: $n = 21$. Wilcoxon rank-sum test; * $P < 0.05$; ** $P < 0.01$. FMT, fecal microbiota transplantation.

Although it is not clear how alterations in the gut microbiota promote beneficial effects in the host, a potential mechanism includes increased production of SCFAs, primarily acetate, propionate, and butyrate, and other organic acids^{26,27}. We therefore performed targeted metabolomics to investigate whether the observed enrichment in genes for SCFA metabolism in the gut microbiome following metformin treatment was paralleled by an increased production of SCFAs. We observed significantly larger increases in fecal propionate and butyrate concentrations in the metformin group, as compared to the placebo group, after 4 months of treatment in men; however, no differences were observed when results from men and women were combined (Fig. 4c). We also observed significantly larger increases in fecal concentrations of lactate and a trend toward a larger increase in fecal concentrations of succinate in the metformin group, as compared to the placebo group, after 4 months of treatment (Fig. 4d).

The gut microbiota is also known to be a major regulator of bile acid metabolism²⁸, which may contribute to its effects on host metabolism. Furthermore, a few studies have indicated a potential role of metformin in altering the bile acid profile^{29,30}, but this link is not well established. Here we investigated the effect of metformin treatment

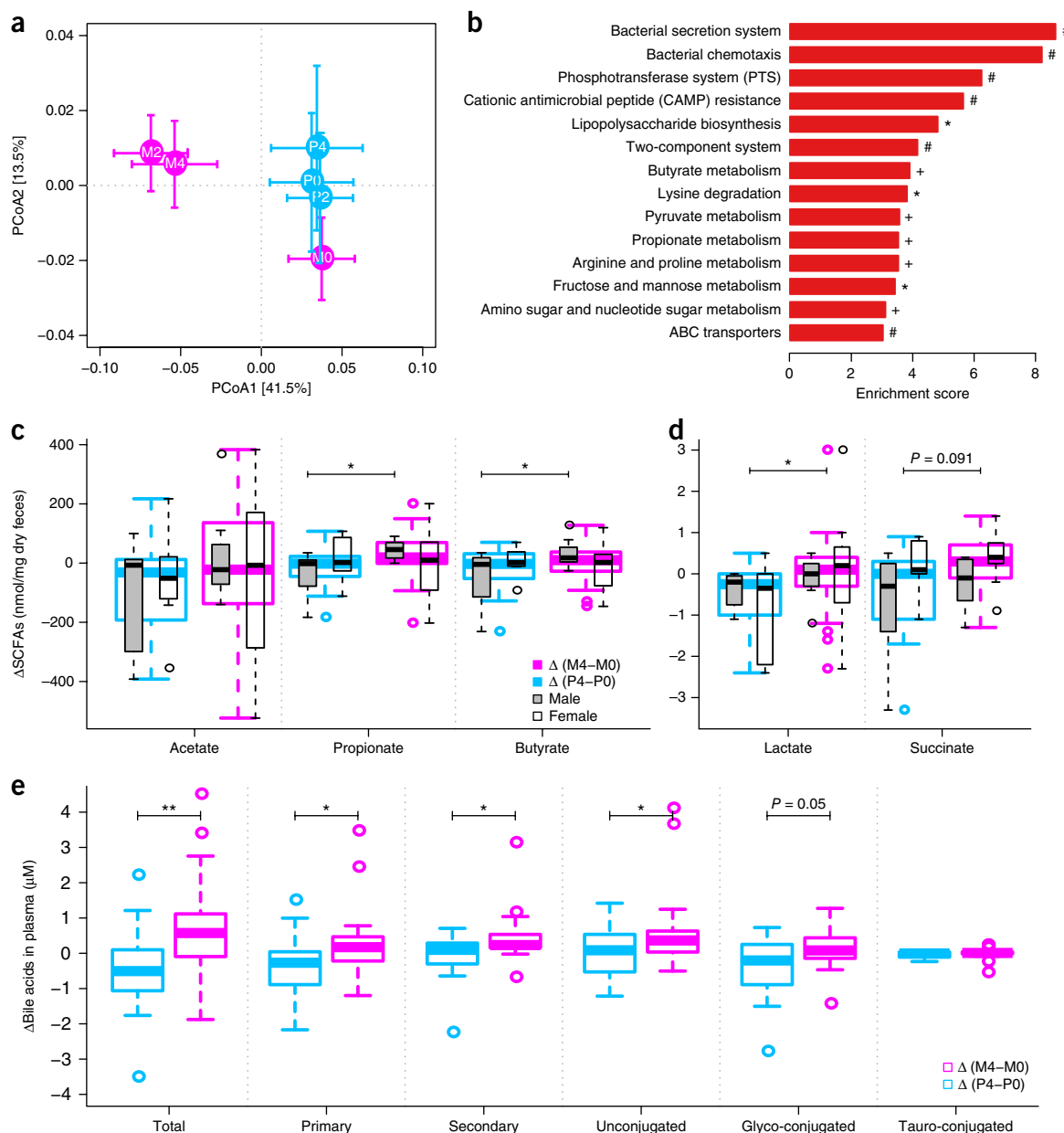


Figure 4 Metformin treatment promotes functional shifts in the gut microbiota. **(a)** Principal coordinate analysis (PCoA) of all KOs that are significantly altered from baseline (P0 and M0) after 2 and 4 months in individuals with T2D randomized to placebo (P2 and P4; $n = 18$) or metformin (M2 and M4; $n = 22$). Adonis test based on 5,000 permutations; $P_{M0 \text{ vs. } M2} = 0.00040$; $P_{M0 \text{ vs. } M4} = 0.0062$. Data are shown as means \pm s.e.m. **(b)** Pathway-enrichment analysis of all significantly altered KOs. Hypergeometric test; *FDR < 0.05; +FDR < 0.01; #FDR < 0.001. **(c–e)** Boxplots (with median) showing changes from baseline (P0 and M0) for fecal concentrations of SCFAs **(c)**, fecal concentrations of lactate and succinate **(d)**, and plasma concentrations of bile acids **(e)** after 4 months in individuals with T2D randomized to placebo (P4; $n = 18$) or metformin (M4; $n = 22$). Wilcoxon rank-sum test; * $P < 0.05$; ** $P < 0.01$.

for 4 months on fecal and plasma bile acid composition. No substantial changes in fecal bile acids were detected following metformin treatment (**Supplementary Fig. 4a**). However, we observed significantly larger increases in plasma bile acid concentrations (total, primary, secondary, and unconjugated) in the metformin group, as compared to the placebo group, after 4 months of treatment (**Fig. 4e**). By using a targeted metagenomic analysis, we showed an increased abundance of *bsh*, genes encoding bile salt hydrolases, after 2 months on metformin (**Supplementary Fig. 4b**). These enzymes are produced by the gut microbiota and catalyze the deconjugation of glycine- or taurine-conjugated bile acids, and thus increases in *bsh* could contribute to the

increased concentrations of unconjugated bile acids. Furthermore, we found a significant negative correlation between the concentrations of unconjugated bile acids and %HbA1c ($\rho = -0.27$, $P < 0.05$), which suggests a possible link between the modulation of bile acid composition and the therapeutic effect of metformin.

Direct effects of metformin on the gut microbiota

To directly investigate how metformin affects the gut microbiota, we cultured fecal samples (obtained before metformin treatment from two participants, donors 13 and 49) in two separate gut-simulator experiments, and exposed the samples to a constant flow of metformin

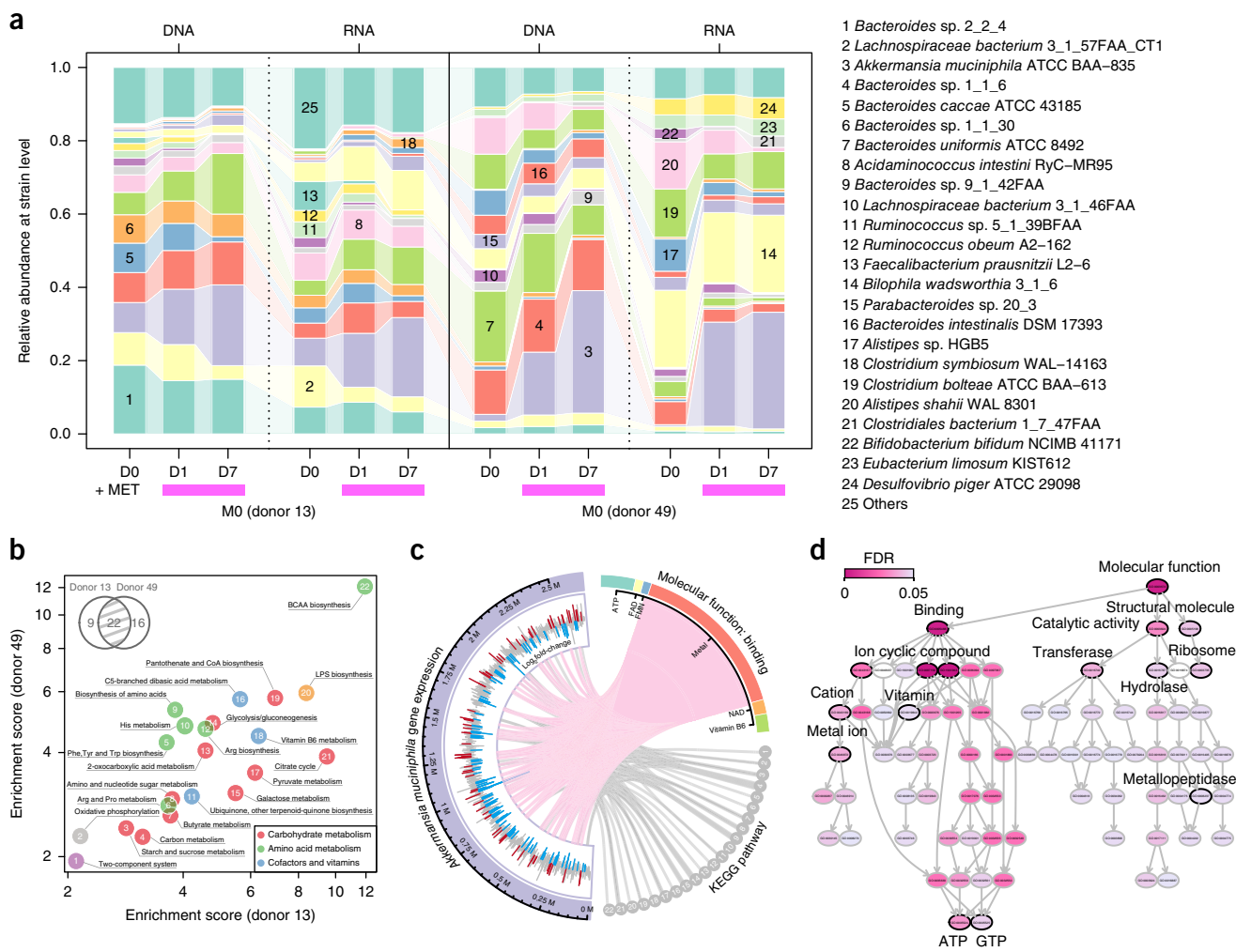


Figure 5 Direct metformin–microbiota interactions identified using an *in vitro* gut simulator. **(a)** Microbial compositional profiling of samples taken from the *in vitro* gut simulator before (D0) and after 1 d and 7 d (D1 and D7) of metformin exposure (+MET). Fecal material from two participants (donors 13 and 49) was used to inoculate the gut simulator in two independent experiments (i.e., the fecal material from the two samples was not pooled). The top ten bacterial strains detected in the samples at each time point are shown. **(b)** Metformin-enriched pathways identified by both metagenomic and metatranscriptomic analyses of samples taken from the *in vitro* gut simulator. Hypergeometric test; FDR < 0.05. Only the 22 pathways affected by metformin exposure in both experiments (inset) are shown. **(c)** Circos plot of KEGG pathway and molecular-function annotations for metformin-regulated genes in *A. muciniphila*. The circular bar plot on the left side indicates metformin-regulated genes along the genome. Red, significantly increased gene expression; blue, significantly decreased; gray, no statistical differences; Wald test; FDR < 0.1. The metformin-regulated genes involved in the 22 pathways shown in **(b)** (gray links) and coding for proteins with metal-binding abilities (pink links) are highlighted. **(d)** Gene ontology (GO) enrichment of all metformin-regulated genes in *A. muciniphila*; GO terms with direct hierarchical parent–child relationships are linked by arrows. Hypergeometric test; FDR < 0.05.

(10 mM) for 1 week. We then profiled the microbiomes by whole-genome shotgun sequencing at both the DNA and RNA level.

Compositional profiling revealed that metformin exposure significantly altered the DNA and RNA abundance of 24 bacterial strains when culturing the feces of donor 13 but of only 4 for the feces of donor 49 (Supplementary Table 5; FDR < 0.05). Donor-specific effects of metformin exposure included, for example, increased RNA abundance of *Bilophila wadsworthia* (donor 13) and increased DNA abundance of *Lachnospiraceae* bacterium (donor 49) (Fig. 5a and Supplementary Table 5). *A. muciniphila* was the only taxon that increased in both DNA and RNA abundance in response to metformin in both samples, and it was also the taxon that increased the most in abundance (Fig. 5a and Supplementary Table 5).

Functional profiling of the combined metagenome and metatranscriptome showed that metformin exposure significantly altered the

abundance of 686 and 909 KOs in samples from donors 13 and 49, respectively (Supplementary Table 6; Wald test, FDR < 0.05). In total, 31 and 38 pathways were enriched after metformin exposure in samples from donors 13 and 49, respectively; of these, 22 enriched pathways were common to both samples (Fig. 5b and Supplementary Table 6; hypergeometric test, FDR < 0.05). Six pathways that were enriched in the metformin-treated samples in the *in vivo* metagenome analysis (see Fig. 4b)—including those for genes involved in LPS synthesis, butyrate and pyruvate metabolism, and two-component systems—were also shown to be enriched by metformin in both gut-simulator experiments (Fig. 5b). In addition, the *in vitro* analysis revealed enrichment of metabolic pathways linked to the metabolism of cofactors and vitamins (Fig. 5b). These results show that although metformin exerts donor-specific taxonomic effects, it induces overlapping microbial functional changes in samples from both donors.

Finally, we performed in-depth transcriptome analyses (using the *in vitro* cultured fecal sample from donor 13) to investigate direct interactions between metformin and individual bacterial species. We first examined the RNA reads that mapped to the gene catalog of *A. muciniphila* (the taxon with the overall highest abundance in this fecal sample; Fig. 5a). We found that nearly 10% (207/2138) of the protein-coding genes in *A. muciniphila* were significantly regulated by metformin; of these, 65% were downregulated by metformin (Supplementary Table 7; FDR < 0.1). Furthermore, 78 of the 207 metformin-regulated genes could be annotated to KOs, and of these, 41 genes mapped to the 22 metformin-enriched pathways common to cultured fecal samples from both donors (Fig. 5c and Supplementary Table 7). By manual annotation, we found that the protein products of 108/207 metformin-regulated genes required cofactors or coenzymes such as ATP, FAD, FMN, metal, NAD, and vitamin B6 (Fig. 5c and Supplementary Table 7); most of the remaining genes (63/99) have not been characterized (Supplementary Table 7). Of particular interest, 81 of the 108 metformin-regulated annotated genes encoded metalloprotein or metal transporters (Fig. 5c and Supplementary Table 7). Gene ontology (GO) analysis of metformin-regulated genes in *A. muciniphila* confirmed that their gene products were enriched in proteins that bind to metal ions in addition to several other cofactors and coenzymes, as well as transferase, hydrolase, ligase, and protein components of ribosomes (Fig. 5d). To address whether those observations were specific to *A. muciniphila*, we also analyzed *B. wadsworthia* (the second most abundant taxon in this cultured fecal sample after metformin treatment; Fig. 5a). According to protein-homology detection, only 14 metformin-regulated genes were orthologous between these two bacteria; however, most annotated metformin-regulated genes in *B. wadsworthia* also encoded metalloproteins (Supplementary Table 7).

DISCUSSION

In this study, we performed a randomized, placebo-controlled, double-blind study in individuals with newly diagnosed T2D on a calorie-restricted diet and showed that metformin, but not calorie restriction, had rapid effects on the composition and function of the gut microbiota in parallel with the reduction of %HbA1c and fasting blood glucose concentrations. Transfer of the microbiota to germ-free mice showed that the metformin-altered microbiota could improve glucose metabolism. Furthermore, transcriptome analyses of feces cultured with metformin *in vitro* in a gut simulator showed that metformin had direct effects on the microbiota and regulated the expression of genes encoding metalloproteins in the gut bacteria.

By using paired samples in our prospective human study, we reduced the effect of interindividual variations, a common issue in previous studies investigating the effect of metformin on the microbiota^{16,17,31}. A further strength of our cohort is that these individuals had been newly diagnosed with T2D and thus were not taking other medications for T2D, and only a small number in each group were taking statins or antihypertensive therapy. We also monitored the dietary intake of the participants before and 4 months after treatment and showed that calorie restriction did not affect the gut microbiome to any great extent in our study; it should be noted that the calorie reduction reported was mild relative to that in earlier studies showing profound changes in the gut microbiome in response to dietary intervention^{22,32}. The design of our study thus enabled us to minimize the effect of major confounding factors known to have an impact on the gut microbiome.

By performing whole-genome shotgun sequencing of fecal samples, we observed dramatic shifts in the composition of the gut microbiota after

2 and 4 months on metformin in individuals with newly diagnosed T2D. Notably, these changes were similar to those observed after 6 months on metformin in a placebo subgroup that switched to metformin 6 months after the study start. In particular, we observed significant changes in *Escherichia* and *Intestinibacter* abundance across all sampling points in the metformin-treated group, a finding that is in agreement with results reported in a cross-sectional study that compared metformin-treated and untreated groups of people with T2D¹⁷. Growth of *E. coli* in an *in vitro* analysis was not affected by metformin. Thus, the effects of metformin on the abundance of *Escherichia* spp. are likely indirect, and possibly, a result of modified bacteria–bacteria interactions or of other physiological and/or environmental changes within the gut upon metformin treatment. We showed that metformin promoted the growth of *B. adolescentis* both *in vivo* (after 2 months in the main study and after 6 months in the switched subgroup, as measured by PTR) and *in vitro* using pure cultures, and also that it increased the abundance of *Bifidobacterium* in the switched subgroup. Supplementation with *B. adolescentis* in a rodent model of the metabolic syndrome has previously been shown to increase insulin sensitivity³³. In our cohort, we also observed a negative correlation between the PTR of *B. adolescentis* and %HbA1c, which suggests that increased growth of this bacterial species could potentially contribute to the antidiabetic effect of metformin.

To observe direct metformin–microbiota interactions, we incubated fecal samples from treatment-naïve participants with metformin in a gut simulator. In this system, we did not observe any significant changes in *E. coli* or *B. adolescentis*. In fact, the only taxon that increased in response to metformin (at both DNA and RNA levels and in samples from two separate donors) was *A. muciniphila*. Metformin has previously been shown to increase the abundance of *A. muciniphila* in rodents on a high-fat diet^{13–15}, and this increased abundance has been linked to improved glucose metabolism^{13,20,21}. However, evidence for a link between metformin and *A. muciniphila* is less clear in humans^{16,17}. We did observe a significant increase in the abundance of *A. muciniphila* over time in the individuals who received metformin for 4 months, but only when we used a targeted analysis. Similarly, a recent study that screened mucin-degrading and butyrate-producing bacteria showed increased abundance of *A. muciniphila* in humans taking metformin¹⁸. In agreement with these observations, we showed that metformin increased the growth of *A. muciniphila* *in vitro* using pure cultures. However, it is likely that the growth of this taxon is affected in humans *in vivo* by factors that differ between individuals, such as fiber³⁴ and polyphenol availability^{35,36}, immune responses^{37,38}, and age^{39,40}. Furthermore, in our study, we did not observe any significant correlations between %HbA1c and *A. muciniphila* abundance, and therefore, cannot conclude that *A. muciniphila* is a major contributor to the beneficial effects of metformin in our human cohort.

By comparing results from the *in vivo* metagenomics analysis and the *in vitro* metagenomics and metatranscriptomics analyses, we noted that metformin promoted consistent shifts in microbial functions, including LPS biosynthesis and SCFA metabolism. Increased LPS biosynthesis might reflect the increased abundance of Gram-negative bacteria such as Proteobacteria, but it was not associated with increased systemic inflammation, because C-reactive protein was unaltered (Table 1). Similarly, enrichment of the LPS biosynthesis pathway without an increase in inflammation has been observed both in humans after bariatric surgery⁴¹ and in prebiotic-treated mice on a high-fat diet⁴². Increased SCFA metabolism in response to metformin has also been predicted in earlier metagenomics

analyses in humans^{17,18}, and in agreement, our targeted metabolomics analysis showed that metformin significantly increased butyrate and propionate in men.

In-depth transcriptome analysis of the effects of metformin on two distantly related bacterial species in the gut simulator showed that most of the metformin-regulated genes encoded metalloproteins or metal transporters. It is unlikely that the transcriptional responses of this subset of genes were due to a growth-induced increase in total transcripts because the majority of these genes were downregulated by metformin. Interestingly, some metals are known to contribute to T2D pathophysiology⁴³, and it has been known for many years that metformin binds to metals⁴⁴. Furthermore, a recent study showed that the effects of metformin on a mammalian liver cell line are dependent on the metal-binding properties of this drug⁴⁴. However, our study, to the best of our knowledge, is among the first to indicate a link between metformin and metal-binding proteins produced by the gut microbiota.

Fecal transfer to germ-free mice resulted in improved glucose tolerance in recipients of metformin-altered microbiota from two out of three donors, with overall substantial improvement of glucose metabolism, thus indicating that metformin-adapted microbiota could contribute to the beneficial effects of metformin on glucose homeostasis. It is not clear why the responses to the metformin-altered microbiota differed between the donors, given that all the donors showed improved glucose tolerance after both 2 and 4 months of metformin treatment. However, there are large interindividual differences in gut-microbiota composition in humans, and the lack of response of microbiota from one donor might be attributable to an incomplete transfer of key species, as has previously been described⁴⁵. Furthermore, the different diets of the recipient mice and the human donors (i.e., high fat as opposed to calorie restriction) would likely exacerbate differences in the gut-microbiota composition between the donors and recipients. The taxa that are successfully transferred to recipient mice will therefore be dependent not only on the composition of the donor gut microbiota, but also on how well the taxa respond to different macronutrients.

There is increasing evidence to indicate that SCFAs and bile acids have a role in the regulation of glucose homeostasis^{26,27,46,47}, and we recently reported that microbiota-produced succinate could improve glucose metabolism by activating intestinal gluconeogenesis in mice⁴⁸. Here we observed metformin-induced alterations in these microbially regulated metabolites, which suggests that they might be partly responsible for the stronger glucose-lowering effect that has been observed when metformin is administered orally as compared with intravenous injection¹¹. It should be noted that we cannot conclude that the major mechanism of action of metformin is through the microbiota. For example, a recent study in mice showed that the phosphorylation of acetyl-CoA carboxylases (ACC) 1 and 2 by AMPK is required to observe the insulin-sensitizing effects of metformin⁵, demonstrating the importance of AMPK/ACC signaling. However, it is possible that the gut microbiota might also act through ACCs, given that we previously showed that diet-induced obesity involved cross-talk between the microbiota, AMPK, and downstream ACC2 phosphorylation⁴⁹.

In summary, our work shows that metformin interacts with different gut bacteria, possibly through the regulation of metal homeostasis. However, additional studies combining untargeted metabolomics and metaproteomics are essential to identify further microbial metabolites or proteins and to determine how they interact with the host targets in improving host metabolism.

METHODS

Methods, including statements of data availability and any associated accession codes and references, are available in the [online version of the paper](#).

Note: Any Supplementary Information and Source Data files are available in the online version of the paper.

ACKNOWLEDGMENTS

We thank C. Arvidsson, S. Nordin-Larsson, C. Wennberg, and U. Enqvist for superb mouse husbandry. The administrative and technical help of J.M. Moreno Navarrete, E. Huertos, M. Sabater, and O. Rovira is also acknowledged. The strain *Akkermansia muciniphila* DSM22959 was kindly provided by W. de Vos (Wageningen University and Helsinki University). The strain *Bifidobacterium adolescentis* L2-32 was kindly provided by K. Scott (The Rowett Institute of Nutrition and Health, University of Aberdeen). Whole-genome shotgun sequencing was performed at the Genomics Core Facility at the Sahlgrenska Academy, University of Gothenburg. The computations for metagenomics analyses were performed on resources provided by the Swedish National Infrastructure for Computing (SNIC) through Uppsala Multidisciplinary Center for Advanced Computational Science (UPPMAX). This study was supported by the Swedish Diabetes Foundation; Swedish Research Council; Swedish Heart Lung Foundation; Torsten Söderberg's Foundation; Göran Gustafsson's Foundation; Inga Britt and Arne Lundberg's Foundation; Swedish Foundation for Strategic Research; Knut and Alice Wallenberg Foundation; the Novo Nordisk Foundation; the regional agreement on medical training and clinical research (ALF) between Region Västra Götaland and Sahlgrenska University Hospital; the Ministerio de Economía y Competitividad (PI11-00214 and PI15/01934); and FEDER funds. CIBEROBN Fisiopatología de la Obesidad y Nutrición is an initiative from the Instituto de Salud Carlos III from Spain. M.P.-F. is funded by the Obra Social Fundación la Caixa fellowship under the Severo Ochoa 2013 program. J.M.M. was supported by the Sara Borrell Fellowship from the Instituto Carlos III, EFSO/Lilly Research Fellowship and Beatriu de Pinós Fellowship from the Agency for Management of University and Research Grants (AGAUR). E.B. is a recipient of ERC Consolidator Grant (European Research Council, Consolidator grant 615362—METABASE).

AUTHOR CONTRIBUTIONS

F.B., J.M.F.-R., V.T., and R.B. conceived and designed the study. E.E., M.P.-F., G.X., J.M.M., D.T., W.R., and J.M.F.-R. recruited cohort individuals and performed the clinical study. H.W., V.T., and F.B. conducted the bioinformatics study, analyzed all results unless otherwise indicated. H.W., V.T., R.P., and F.B. wrote the paper. M.T.K. performed the *in vitro* gut simulator and bacterial growth experiments. R.C. and L.M.-H. performed and analyzed the fecal microbiota transplantation experiments. M. Ståhlman performed the metabolomics experiments. M. Serino and V.T. extracted the bacterial DNA and discussed the results. L.M.O. and V.T. extracted the bacterial RNA and coordinated the metagenomics and metatranscriptomics sequencing. All authors commented on the manuscript.

COMPETING FINANCIAL INTERESTS

The authors declare no competing financial interests.

Reprints and permissions information is available online at <http://www.nature.com/reprints/index.html>. Publisher's note: Springer Nature remains neutral with regard to jurisdictional claims in published maps and institutional affiliations.

- Nathan, D.M. *et al.* Medical management of hyperglycemia in type 2 diabetes: a consensus algorithm for the initiation and adjustment of therapy: a consensus statement of the American Diabetes Association and the European Association for the Study of Diabetes. *Diabetes Care* **32**, 193–203 (2009).
- Pernicova, I. & Korbonits, M. Metformin—mode of action and clinical implications for diabetes and cancer. *Nat. Rev. Endocrinol.* **10**, 143–156 (2014).
- Zhou, G. *et al.* Role of AMP-activated protein kinase in mechanism of metformin action. *J. Clin. Invest.* **108**, 1167–1174 (2001).
- Shaw, R.J. *et al.* The kinase LKB1 mediates glucose homeostasis in liver and therapeutic effects of metformin. *Science* **310**, 1642–1646 (2005).
- Fullerton, M.D. *et al.* Single phosphorylation sites in Acc1 and Acc2 regulate lipid homeostasis and the insulin-sensitizing effects of metformin. *Nat. Med.* **19**, 1649–1654 (2013).
- Foretz, M. *et al.* Metformin inhibits hepatic gluconeogenesis in mice independently of the LKB1/AMPK pathway via a decrease in hepatic energy state. *J. Clin. Invest.* **120**, 2355–2369 (2010).
- Madiraju, A.K. *et al.* Metformin suppresses gluconeogenesis by inhibiting mitochondrial glycerol phosphate dehydrogenase. *Nature* **510**, 542–546 (2014).
- Miller, R.A. *et al.* Biguanides suppress hepatic glucagon signalling by decreasing production of cyclic AMP. *Nature* **494**, 256–260 (2013).

9. McCreight, L.J., Bailey, C.J. & Pearson, E.R. Metformin and the gastrointestinal tract. *Diabetologia* **59**, 426–435 (2016).
10. Duca, F.A. *et al.* Metformin activates a duodenal Ampk-dependent pathway to lower hepatic glucose production in rats. *Nat. Med.* **21**, 506–511 (2015).
11. Stepanyk, D., Friedman, M., Raz, I. & Hoffman, A. Pharmacokinetic-pharmacodynamic analysis of the glucose-lowering effect of metformin in diabetic rats reveals first-pass pharmacodynamic effect. *Drug Metab. Dispos.* **30**, 861–868 (2002).
12. Buse, J.B. *et al.* The primary glucose-lowering effect of metformin resides in the gut, not the circulation. Results from short-term pharmacokinetic and 12-week dose-ranging studies. *Diabetes Care* **39**, 198–205 (2016).
13. Shin, N.R. *et al.* An increase in the *Akkermansia* spp. population induced by metformin treatment improves glucose homeostasis in diet-induced obese mice. *Gut* **63**, 727–735 (2014).
14. Zhang, X. *et al.* Modulation of gut microbiota by berberine and metformin during the treatment of high-fat diet-induced obesity in rats. *Sci. Rep.* **5**, 14405 (2015).
15. Lee, H. & Ko, G. Effect of metformin on metabolic improvement and gut microbiota. *Appl. Environ. Microbiol.* **80**, 5935–5943 (2014).
16. Karlsson, F.H. *et al.* Gut metagenome in European women with normal, impaired and diabetic glucose control. *Nature* **498**, 99–103 (2013).
17. Forslund, K. *et al.* Disentangling type 2 diabetes and metformin treatment signatures in the human gut microbiota. *Nature* **528**, 262–266 (2015).
18. de la Cuesta-Zuluaga, J. *et al.* Metformin is associated with higher relative abundance of mucin-degrading *Akkermansia muciniphila* and several short-chain fatty acid-producing microbiota in the gut. *Diabetes Care* **40**, 54–62 (2017).
19. Karlsson, F.H., Nookaew, I. & Nielsen, J. Metagenomic data utilization and analysis (MEDUSA) and construction of a global gut microbial gene catalogue. *PLoS Comput. Biol.* **10**, e1003706 (2014).
20. Everard, A. *et al.* Cross-talk between *Akkermansia muciniphila* and intestinal epithelium controls diet-induced obesity. *Proc. Natl. Acad. Sci. USA* **110**, 9066–9071 (2013).
21. Plovier, H. *et al.* A purified membrane protein from *Akkermansia muciniphila* or the pasteurized bacterium improves metabolism in obese and diabetic mice. *Nat. Med.* **23**, 107–113 (2017).
22. Dao, M.C. *et al.* *Akkermansia muciniphila* and improved metabolic health during a dietary intervention in obesity: relationship with gut microbiome richness and ecology. *Gut* **65**, 426–436 (2016).
23. Park, S.K., Kim, M.S., Roh, S.W. & Bae, J.W. *Blautia stercoris* sp. nov., isolated from human faeces. *Int. J. Syst. Evol. Microbiol.* **62**, 776–779 (2012).
24. Korem, T. *et al.* Growth dynamics of gut microbiota in health and disease inferred from single metagenomic samples. *Science* **349**, 1101–1106 (2015).
25. Kanehisa, M. & Goto, S. KEGG: kyoto encyclopedia of genes and genomes. *Nucleic Acids Res.* **28**, 27–30 (2000).
26. Wong, J.M., de Souza, R., Kendall, C.W., Emam, A. & Jenkins, D.J. Colonic health: fermentation and short chain fatty acids. *J. Clin. Gastroenterol.* **40**, 235–243 (2006).
27. Koh, A., De Vadder, F., Kovatcheva-Datchary, P. & Bäckhed, F. From dietary fiber to host physiology: short-chain fatty acids as key bacterial metabolites. *Cell* **165**, 1332–1345 (2016).
28. Ridlon, J.M., Harris, S.C., Bhowmik, S., Kang, D.J. & Hylemon, P.B. Consequences of bile salt biotransformations by intestinal bacteria. *Gut Microbes* **7**, 22–39 (2016).
29. Caspary, W.F. *et al.* Alteration of bile acid metabolism and vitamin-B12-absorption in diabetics on biguanides. *Diabetologia* **13**, 187–193 (1977).
30. Scarpello, J.H., Hodgson, E. & Howlett, H.C. Effect of metformin on bile salt circulation and intestinal motility in type 2 diabetes mellitus. *Diabet. Med.* **15**, 651–656 (1998).
31. Zhernakova, A. *et al.* Population-based metagenomics analysis reveals markers for gut microbiome composition and diversity. *Science* **352**, 565–569 (2016).
32. Cotillard, A. *et al.* Dietary intervention impact on gut microbial gene richness. *Nature* **500**, 585–588 (2013).
33. Chen, J., Wang, R., Li, X.F. & Wang, R.L. *Bifidobacterium adolescentis* supplementation ameliorates visceral fat accumulation and insulin sensitivity in an experimental model of the metabolic syndrome. *Br. J. Nutr.* **107**, 1429–1434 (2012).
34. Desai, M.S. *et al.* A dietary fiber-deprived gut microbiota degrades the colonic mucus barrier and enhances pathogen susceptibility. *Cell* **167**, 1339–1353.e21 (2016).
35. Roopchand, D.E. *et al.* Dietary polyphenols promote growth of the gut bacterium *Akkermansia muciniphila* and attenuate high-fat diet-induced metabolic syndrome. *Diabetes* **64**, 2847–2858 (2015).
36. Anhê, F.F. *et al.* A polyphenol-rich cranberry extract protects from diet-induced obesity, insulin resistance and intestinal inflammation in association with increased *Akkermansia* spp. population in the gut microbiota of mice. *Gut* **64**, 872–883 (2015).
37. Greer, R.L. *et al.* *Akkermansia muciniphila* mediates negative effects of IFN γ on glucose metabolism. *Nat. Commun.* **7**, 13329 (2016).
38. Zhang, H., Sparks, J.B., Karyala, S.V., Settlage, R. & Luo, X.M. Host adaptive immunity alters gut microbiota. *ISME J.* **9**, 770–781 (2015).
39. Collado, M.C., Derrien, M., Isolauri, E., de Vos, W.M. & Salminen, S. Intestinal integrity and *Akkermansia muciniphila*, a mucin-degrading member of the intestinal microbiota present in infants, adults, and the elderly. *Appl. Environ. Microbiol.* **73**, 7767–7770 (2007).
40. Kong, F. *et al.* Gut microbiota signatures of longevity. *Curr. Biol.* **26**, R832–R833 (2016).
41. Tremaroli, V. *et al.* Roux-en-Y gastric bypass and vertical banded gastroplasty induce long-term changes on the human gut microbiome contributing to fat mass regulation. *Cell Metab.* **22**, 228–238 (2015).
42. Everard, A. *et al.* Microbiome of prebiotic-treated mice reveals novel targets involved in host response during obesity. *ISME J.* **8**, 2116–2130 (2014).
43. Fernández-Real, J.M. & Manco, M. Effects of iron overload on chronic metabolic diseases. *Lancet Diabetes Endocrinol.* **2**, 513–526 (2014).
44. Logie, L. *et al.* Cellular responses to the metal-binding properties of metformin. *Diabetes* **61**, 1423–1433 (2012).
45. Wahlström, A. *et al.* Induction of farnesoid X receptor signaling in germ-free mice colonized with a human microbiota. *J. Lipid Res.* **58**, 412–419 (2017).
46. Wahlström, A., Sayin, S.I., Marschall, H.U. & Bäckhed, F. Intestinal crosstalk between bile acids and microbiota and its impact on host metabolism. *Cell Metab.* **24**, 41–50 (2016).
47. Schaap, F.G., Trauner, M. & Jansen, P.L. Bile acid receptors as targets for drug development. *Nat. Rev. Gastroenterol. Hepatol.* **11**, 55–67 (2014).
48. De Vadder, F. *et al.* Microbiota-produced succinate improves glucose homeostasis via intestinal gluconeogenesis. *Cell Metab.* **24**, 151–157 (2016).
49. Bäckhed, F., Manchester, J.K., Semenkovich, C.F. & Gordon, J.I. Mechanisms underlying the resistance to diet-induced obesity in germ-free mice. *Proc. Natl. Acad. Sci. USA* **104**, 979–984 (2007).

ONLINE METHODS

Clinical study design. 40 individuals with T2D were recruited and randomized (using a computational random generator Aleator) to treatment with metformin ($n = 22$) or placebo ($n = 18$) for 4 months. Metformin (Acyfabrik, Madrid, Spain) was started at a dose of 425 mg/d and increased progressively during the first week to reach 1,700 mg/d (in three doses). We instructed both groups to maintain a reduction in daily caloric intake of 500 kcal during the entire treatment. We recommended a hypocaloric diet containing 25 kcal/kg or 20 kcal/kg and used a validated food-frequency questionnaire⁵⁰. The composition of the diet was 15% protein, 30% fat (<10% saturated fat), 55% carbohydrates, and 20–25 g dietary fiber (**Supplementary Table 1**). Lifestyle changes were also suggested, including regular physical activity (150 min/week). We collected both fecal and plasma samples at baseline and at 2 and 4 months after treatment. A subgroup of those on placebo switched to metformin treatment after 6 months of dietary intervention (850 or 1,700 mg/d, $n = 13$); we obtained fecal and plasma samples from these individuals after a further 6 months. People in this group were not randomly selected, but had agreed to be treated with metformin. Compliance and side effects were monitored at each visit.

Inclusion criteria were: (i) aged between 18 and 65 years; (ii) T2D diagnosis in the previous 6 months, as defined by the American Diabetes Association Criteria⁵¹; (iii) absence of systemic and metabolic disease other than T2D, and absence of infection within the previous month; (iv) absence of diet or medication that might interfere with glucose homeostasis, such as glucocorticoids or antibiotics in the previous 3 months; and (v) HbA1c lower than 9%.

Exclusion criteria were: (i) clinically significant major systemic disease, including malignancy; (ii) clinical evidence of hemoglobinopathies or anemia; (iii) history of drug or alcohol abuse, defined as >80 g/d in men and >40 g/d in women; (iv) acute major cardiovascular event in the previous 6 months; (v) acute illnesses or current evidence of acute or chronic inflammatory or infective disease; and (vi) mental illness rendering the participants unable to understand the nature, scope, and possible consequences of the study.

All individuals gave written informed consent. The experimental protocol was approved by the Ethics Committee and the Committee for Clinical Investigation of the Hospital Universitari Dr. Josep Trueta (Girona, Spain). We certify that all applicable institutional regulations concerning the ethical use of information and samples from human volunteers were followed during this research. Complete clinical trial registration is deposited in the EU clinical trials register (EudraCT number 2010-022394-34).

Extraction of fecal genomic DNA and whole-genome shotgun sequencing.

Fecal genomic DNA was extracted from 100 mg of frozen stools using the QIAamp DNA mini stool kit (Qiagen, Courtaboeuf, France) following repeated bead-beating (6,500 r.p.m., 3×30 s). The DNA was extracted from 131 fecal samples, obtained from the participants at three different time points during the study ($n = 118$; two fecal samples were not obtained) and from 13 participants additionally sampled 6 months after switch to metformin treatment. DNA fragments of approximately 300 bp were sequenced on an Illumina NextSeq 500 instrument (150 bp; paired-end) at Genomics Core Facility at the Sahlgrenska Academy, University of Gothenburg.

Metagenomics analyses. We obtained a total of 941 Gb of raw paired-end reads. The taxonomic and KO composition was obtained by using an updated version of the MEDUSA pipeline¹⁹, in which the raw reads were trimmed by FASTX (http://hannonlab.cshl.edu/fastx_toolkit/); with a quality threshold of 20 bp and minimum length of 35 bp), filtered to remove human reads (version hg19), and then mapped to bacterial gene and genome catalogs using Bowtie2 (ref. 52). An additional filter was applied during the mapping process containing reads with at least 95% identity to obtain high-quality reads. The mean mapping rates for the genome and gene catalogs were 36.6% and 64.6%, respectively (**Supplementary Table 2**). The obtained taxonomic composition and KO profile matrix were further analyzed by DESeq2 package⁵³. Pathway-enrichment analyses are based on KEGG annotation²⁵ and hypergeometric test using goseq⁵⁴. The beta diversity and PCoA analysis were calculated on the basis of the relative abundance of all significant KOs (further transformed by the square root to reduce the influence of dominant KOs, as suggested previously⁵⁵) using phyloseq (version 1.12.2)⁵⁶. Genus-to-genus

coabundance network analysis was based on Spearman correlation. Only genera present in at least 80% of samples were used for correlation analysis, and only connections with a rho value larger than 0.6 or smaller than -0.6 were used for network building and visualization, on the basis of igraph⁵⁷. For the estimation of PTRs, metagenomic reads were mapped to a local genome database containing ~200 common human bacterial strains, using the software PTRC²⁴. For the analysis of bile salt hydrolase (*bsh*) genes, a local gene database containing all available *bsh* genes was constructed by blasting⁵⁸ against NCBI reference genes⁵⁹, MEDUSA gene catalog¹⁹, and the integrated gene catalog for human microbiome (IGC)⁶⁰ using 16 randomly selected seed *bsh* genes (gi: 169212173, 47121626, 488267184, 489835719, 491501450, 491807128, 499725619, 503743756, 524844235, 558633790, 654788256, 753801014, 759977951, 814507153, 823277295 and 933135484). The local *bsh* gene database was then used for targeted reads screening on the basis of the MEDUSA pipeline¹⁹.

Targeted metabolomics analyses. Fecal SCFAs were measured using gas chromatography coupled to mass spectrometry detection (GC-MS), as described previously⁶¹. In brief, approximately 50–250 mg of feces were mixed with internal standards, added to glass vials and freeze-dried. All samples were then acidified with HCl, and SCFAs were extracted with two rounds of diethyl ether extraction. The organic supernatant was collected, the derivatization agent *N*-tert-butylidimethylsilyl-*N*-methyltrifluoroacetamide (Sigma-Aldrich, Stockholm, Sweden) was added, and samples were incubated overnight. SCFAs were quantified with a 7090A gas chromatograph coupled to a 5975C mass spectrometer (Agilent Technologies 5975C, Santa Clara, CA). SCFA standards were obtained from Sigma-Aldrich (Stockholm, Sweden).

Bile acids were analyzed using ultra-performance liquid chromatography coupled to tandem mass spectrometry (UPLC-MS/MS), as described before⁴¹. Briefly, bile acids from plasma were extracted using protein precipitation with ten volumes of methanol containing internal standards. After mixing and centrifugation, the samples were evaporated and reconstituted in 200 μ l of methanol:water (1:1) for analysis. For feces, about 50 mg of stool samples were placed in a 2-ml polypropylene tube together with six ceramic beads (3 mm; Retsch GmbH, Haan, Germany) and 500 μ l of internal standard containing methanol. Stools were homogenized and centrifuged, and the supernatant was diluted ten times in methanol:water (1:1) before analysis. Bile acids were separated using a Kinetex C18 column (2.1 \times 100 mm with 1.7- μ m particles) (Phenomenex, Torrance, CA, USA) kept at 60 °C. The mobile phases consisted of water with 7.5-mM ammonium acetate and 0.019% formic acid (pH 4.5) as mobile phase A, and acetonitrile with 0.1% formic acid as phase B. A QTRAP 5500 instrument (Sciex, Toronto, Canada) was used for detection using multiple-reaction monitoring in negative mode. Bile acid standards were obtained from Sigma-Aldrich (Stockholm, Sweden), CDN Isotopes (Quebec, Canada), and Toronto Research Chemicals (Downsview, Ontario, Canada).

Animal procedures. Animal procedures were approved by the Gothenburg Animal Ethics Committee. For the fecal-microbiota transplant experiments, we used 10- to 12-week-old male Swiss Webster germ-free mice. Mice were kept in individually ventilated cages (ISOcage N System, Tecniplast, Buguggiate, Italy) with a maximum of five mice per cage. Water was given *ad libitum*. 500 mg of frozen stools obtained at baseline (M0) and 4 months after metformin treatment (M4) from three individuals were suspended in 5 ml of reduced PBS buffer containing 0.2 g/liter Na₂S and 0.5 g/liter cysteine as reducing agents. The three donors were chosen from the metformin arm of the randomized clinical study who showed a reduction in %HbA1c after 2 and 4 months of metformin treatment, and the individual stool samples were not pooled. The germ-free mice were randomized into two groups and colonized by oral gavage with 200 μ l of M0/M4 fecal slurry from each donor. The mice were fed an irradiated high-fat diet (40% kcal fat, TD09683, Harlan Teklad) for 1 week before and during the 18 d of colonization. Body composition was determined with an EchoMRI instrument (EchoMRI) 1 d after colonization and at the end of the experiment. Insulin was measured with a kit from Crystal Chem (Downers Grove, IL) according to the manufacturer's protocol, and an intraperitoneal glucose-tolerance test was performed at the end of the experiment, as previously described⁶². The investigators were not blinded to the group allocation. No mice were excluded from this study.

In vitro bacterial growth experiments. Precultures of *B. adolescentis* L2-32 and *E. coli* were inoculated anaerobically in a Coy chamber (5% hydrogen, 10% carbon dioxide, and 85% nitrogen) as single colonies in 7 ml of brain-heart infusion (BHI) medium containing (in g/liter) yeast extract (5), cellobiose (1), maltose (1), cysteine (0.5), and hemin (0.01). For *A. muciniphila*, modified BHI broth was used, into which cysteine (0.05%) and type II mucin (1%) were added. Before inoculation, the modified medium was filtered through a 0.22- μ m filter. After incubation for 14 h, each preculture was inoculated in freshly prepared BHI broth or modified BHI broth with or without metformin in a 24-well plate or 96-well microplate at a concentration (v/v) of 0.5% *E. coli* or 1% *B. adolescentis* in a volume of 2.5 ml and 2% *A. muciniphila* in a volume of 300 μ l. The effect of metformin on bacterial-growth kinetics was analyzed in a CLARIOstar microplate reader equipped with atmospheric control unit (BMG Labtech) by following the optical density (OD₆₀₀). The atmospheric oxygen concentration was reduced to 0.1% and was maintained with nitrogen as ground gas. The growth-curve data over 10 h for *E. coli* and *B. adolescentis* and 30 h for *A. muciniphila* were analyzed using MARS data-analysis software (BMG Labtech.).

In vitro gut simulator. A simulated human intestinal redox model (SHRIM) was used to explore the effect of metformin on a stabilized gut microbial community *in vitro*. SHRIM is a two-chamber fermenter with an anaerobic luminal chamber (250 ml) and an oxygen feeder (100 ml), which are separated by a Nafion Membrane N115 (DuPont, USA; diameter 2.5 cm) and continuously purged with nitrogen and oxygen, respectively. The luminal chamber was continuously stirred at 250 r.p.m. and kept at 37 °C. The oxygen feeder contained 100-mM potassium phosphate buffer. The luminal chamber was seeded with 250 ml of feed containing: (in g/liter) arabinogalactan (1.0), pectin (2.0), xylose (1.5), starch (3.0), glucose (0.4), yeast extract (3.0), peptone (1.0), mucin type II (4.0), and cysteine (0.5). To simulate digestion processes, the feed was acidified to around pH 2 with 6-M HCl, and neutralized with simulated pancreatic juice to a pH of around 6.9. The simulated pancreatic juice contained: (in g/liter) NaHCO₃ (12.5), Oxgall bile salts (6.0), and pancreatin (0.9). The feed and pancreatic juice mix (70:30), referred to as SHRIM feed, was kept anaerobic by continuously purging with nitrogen⁶³. The SHRIM feed was fed continuously to the luminal chamber at a rate giving a retention time of around 24 h, and pH was maintained between 6.9 and 6.6 with pH controller and dosing Pump (Black stone BL7912, Hanna Instruments, UK).

The SHRIM system was inoculated with an aliquot of the M0 fecal sample from each donor individually. A preculture was prepared anaerobically in a Coy chamber (5% hydrogen, 10% carbon dioxide, and 85% nitrogen) by adding 2% fecal material to 5 ml of BHI broth as described above. The preculture was incubated for 3 h at 37 °C, and 2% of the pre-culture was seeded into the luminal compartment of the SHRIM.

Analysis of metagenome and metatranscriptome of the microbial community in the *in vitro* gut simulator. After 1 week of stabilization, the microbial community was challenged with 10-mM metformin continuously, and samples (2 \times 1 ml) were taken at baseline (time zero) and then daily for 1 week. After centrifugation at 16,000 r.p.m. for 2 min at 4 °C, the cellular pellet was suspended in 1 ml of Tris-EDTA buffer (10-mM Tris, 1-mM EDTA pH 7.5), and 500- μ l aliquots were used for DNA and RNA extractions. Total DNA was extracted by repeated bead-beating, as previously described⁶⁴. Total RNA was extracted according to the Macaloid isolation protocol using the Phase Lock Gel Heavy tubes (5 Prime GmbH) and the RNeasy mini kit with on-column DNaseI treatment (Qiagen) for purification, as previously described^{65,66}.

Whole-genome shotgun sequencing was performed both on isolated DNA and RNA from the gut simulator at baseline and after 1 d and 7 d of metformin treatment on Illumina NextSeq 500 instrument at Genomics Core Facility at the Sahlgrenska Academy, University of Gothenburg. An average of 21.6 million paired-end 150-bp DNA reads and 35.2 million paired-end 75-bp RNA reads from both donors were generated for metagenome and metatranscriptome analysis, respectively. Libraries for metagenome sequencing were prepared as mentioned above. Libraries for metatranscriptome sequencing were prepared from rRNA-depleted total RNA using the TruSeq Stranded Total RNA Library Preparation kit (Illumina). rRNA was depleted using the Ribo-Zero rRNA Removal Kit for Gram-positive and Gram-negative bacteria (Illumina).

Then the MEDUSA pipeline¹⁹ was used to obtain the taxonomical composition and functional KO profiles, as described for the metagenomics analysis. In addition, to analyze the gene expression profile of *A. muciniphila* and *B. wadsworthia*, a local gene database containing only genes from those two bacteria was downloaded from NCBI (accession number NC_010655.1 and NZ_ADPC0000000.2, respectively). The circo plot was produced using R package circlize⁶⁷. GO enrichment was performed using R package STRINGdb (version 1.10.0)⁶⁸.

Statistical analysis. All statistical analyses were performed in the R environment⁶⁹. A power of 97% was obtained using pwr package⁷⁰ for this study, on the basis of 22 individuals, with paired design, 5% significance, and an estimated effect size of 0.87 for metformin in improving fasting blood glucose⁷¹. Because the primary aim of our randomized controlled study was to investigate the effect of metformin on the composition and function of the gut microbiota, we did not perform a power calculation for the placebo relative to metformin groups, because the effect size of metformin together with a calorie-restricted diet on the microbiota was previously unknown. For animal tests, sample size was chosen on the basis of our earlier experience and no statistical test was used to predetermine sample size.

Wald test with paired design implemented in DESeq2 (ref. 53) was used for differential abundance analyses for all count data (in the case of both metagenomics and metatranscriptomics). The Spearman's rank-order correlation was used to determine the strength and direction of the monotonic relationships between two variables unless strong collinearity was observed, in which case the Pearson product-moment correlation was calculated. Multivariate analysis with the Adonis test was performed on the basis of 5,000 permutations, using vegan⁷². Statistical testing for bacterial growth rates was examined by two-way ANOVA with repeated measures based on six technical replicates. Changes in SCFA concentrations between the metformin and placebo groups were compared by linear regression adjusted for BMI, gender, and fiber intake; the same procedure was used for bile acids, except the data were adjusted for total calorie intake instead of fiber intake. Otherwise, two-tailed Wilcoxon rank-sum tests or Wilcoxon signed-rank tests were used throughout the study, depending on whether the samples were paired. Raw *P* values were adjusted by the Benjamini-Hochberg method⁷³ with a false discovery rate of 5%, unless indicated otherwise.

Data availability. Sequence data are available for download from the Sequence Read Archive with accession number PRJNA361402.

50. Vioque, J. *et al.* Reproducibility and validity of a food frequency questionnaire among pregnant women in a Mediterranean area. *Nutr. J.* **12**, 26 (2013).
51. American Diabetes Association. Diagnosis and classification of diabetes mellitus. *Diabetes Care* **33** (Suppl. 1), S62-S69 (2010).
52. Langmead, B. & Salzberg, S.L. Fast gapped-read alignment with Bowtie 2. *Nat. Methods* **9**, 357-359 (2012).
53. Love, M.I., Huber, W. & Anders, S. Moderated estimation of fold change and dispersion for RNA-seq data with DESeq2. *Genome Biol.* **15**, 550 (2014).
54. Young, M.D., Wakefield, M.J., Smyth, G.K. & Oshlack, A. Gene ontology analysis for RNA-seq: accounting for selection bias. *Genome Biol.* **11**, R14 (2010).
55. Kindt, R. & Coe, R. *Tree diversity analysis. A manual and software for common statistical methods for ecological and biodiversity studies* (World Agroforestry Centre, Nairobi, Kenya, 2005).
56. McMurdie, P.J. & Holmes, S. phyloseq: an R package for reproducible interactive analysis and graphics of microbiome census data. *PLoS One* **8**, e61217 (2013).
57. Csárdi, G. & Nepusz, T. The igraph software package for complex network research. *InterJournal. Complex Syst.* **1695**, 1695 (2006).
58. Altschul, S.F., Gish, W., Miller, W., Myers, G.W. & Lipman, D.J. Basic local alignment search tool. *J. Mol. Biol.* **215**, 403-410 (1990).
59. Tatusova, T., Ciufu, S., Fedorov, B., O'Neill, K. & Tolstoy, I. RefSeq microbial genomes database: new representation and annotation strategy. *Nucleic Acids Res.* **42**, D553-D559 (2014).
60. Li, J. *et al.* An integrated catalog of reference genes in the human gut microbiome. *Nat. Biotechnol.* **32**, 834-841 (2014).
61. Wichmann, A. *et al.* Microbial modulation of energy availability in the colon regulates intestinal transit. *Cell Host Microbe* **14**, 582-590 (2013).
62. Lee, Y.S. *et al.* Insulin-like peptide 5 is a microbially regulated peptide that promotes hepatic glucose production. *Mol. Metab.* **5**, 263-270 (2016).
63. Van den Abbeele, P. *et al.* Microbial community development in a dynamic gut model is reproducible, colon region specific, and selective for *Bacteroidetes* and *Clostridium* cluster IX. *Appl. Environ. Microbiol.* **76**, 5237-5246 (2010).

64. Salonen, A. *et al.* Comparative analysis of fecal DNA extraction methods with phylogenetic microarray: effective recovery of bacterial and archaeal DNA using mechanical cell lysis. *J. Microbiol. Methods* **81**, 127–134 (2010).
65. Murphy, N.R. & Hellwig, R.J. Improved nucleic acid organic extraction through use of a unique gel barrier material. *Biotechniques* **21**, 934–936, 938–939 (1996).
66. Zoetendal, E.G. *et al.* Isolation of RNA from bacterial samples of the human gastrointestinal tract. *Nat. Protoc.* **1**, 954–959 (2006).
67. Gu, Z., Gu, L., Eils, R., Schlesner, M. & Brors, B. circlize Implements and enhances circular visualization in R. *Bioinformatics* **30**, 2811–2812 (2014).
68. Franceschini, A. *et al.* STRING v9.1: protein-protein interaction networks, with increased coverage and integration. *Nucleic Acids Res.* **41**, D808–D815 (2013).
69. Team, R.C.R. A language and environment for statistical computing. R Foundation for Statistical Computing, Vienna, Austria. <http://www.R-project.org/> (2015).
70. Champely, S. pwr: Basic Functions for Power Analysis. R package version 1.1-3. <http://CRAN.R-project.org/package=pwr> (2015).
71. Leucht, S., Helfer, B., Gartlehner, G. & Davis, J.M. How effective are common medications: a perspective based on meta-analyses of major drugs. *BMC Med.* **13**, 253 (2015).
72. Oksanen, J. *et al.* vegan: Community Ecology Package. R package version 2.2-1 <http://CRAN.R-project.org/package=vegan> (2015).
73. Benjamini, Y. & Hochberg, Y. Controlling the false discovery rate: a practical and powerful approach to multiple testing. *J. R. Stat. Soc. B* **57**, 289–300 (1995).